

---

**Escherichia coli ribosome unfolding in low  $Mg^{2+}$  solutions observed by laser Raman spectroscopy and electron microscopy**

---

T.C.King, T.Rucinsky and D.Schlessinger

Department of Microbiology and Immunology, Washington University School of Medicine, St. Louis, MO 63110, and

F.Milanovich

University of California, Lawrence Livermore Laboratory, Livermore, CA 94550, USA

---

Received 15 September 1980

---

**ABSTRACT**

Ribosomes unfolded by the removal of  $Mg^{2+}$  at 25°C were studied by Raman spectroscopy and electron microscopy. Raman spectra showed a reduction in the  $813\text{ cm}^{-1}$  phosphodiester signal of 30S and 50S ribosomes compared to intact ribosomes, suggesting that a fraction of the ribose moieties had shifted from the 3' endo (ordered) to the 3' exo (disordered) conformation.

The maximum diameters of unfolded 30S and 50S ribosomes, judged by electron microscopy, were 1.8 and 2.5-fold greater, respectively, than those of intact ribosomes. Most unfolded 30S ribosomes had three distinct structural domains and appeared "Y-shaped"; whereas most unfolded 50S ribosomes had four distinct domains and appeared "X-shaped". When ribosomes were partially unfolded (by brief exposure to 0.04 mM  $Mg^{2+}$  or EDTA), several possible intermediates in the unfolding process were observed.

Both the shapes of particles and their Raman spectra reached the same final state in 0.04 mM  $Mg^{2+}$ , where more than 50% of the rRNA phosphates are discharged by  $Mg^{2+}$ , as in 10 mM EDTA, where less than 1% are discharged.

**INTRODUCTION**

Since the earliest studies of ribosomes,  $Mg^{2+}$  was known to be required for their stability. Gesteland (1) showed that when EDTA was used to remove  $Mg^{2+}$  from ribosomes, the particles sedimented more slowly. He also presented evidence that discrete intermediates in the unfolding reaction exist. However, the observed changes in sedimentation coefficient gave little information about specific structural changes during unfolding. Subsequently, ribosome unfolding has been studied with many different techniques. Investigators have characterized some of the hydrodynamic parameters of unfolded ribosomes, such as viscosity and diffusion constant. These studies generally reinforce conclusions drawn from Gesteland's sedimentation analysis, but they do not yield additional information about the conformation of unfolded ribosomes. The ultraviolet absorption and circular dichroism of unfolded ribosomes have provided some information about the unfolding reaction at the molecular level (4-6), but the precise

interpretation of some of these data is uncertain.

In this study we have applied Raman spectroscopy and electron microscopy (EM) to the phenomenon of ribosome unfolding. Since Raman spectroscopy has already provided important information about the conformation of 5S rRNA (7), it was possible that it might yield information about molecular changes during the unfolding of ribosomes. EM permits the evaluation of the size and shape of unfolded ribosomes and the identification of any intermediates in the unfolding process.

### METHODS

Ribosomes were prepared by conventional means from *E. coli* strain D10 (1,8). 30S and 50S subunits were separated by zonal centrifugation and concentrated by ethanol precipitation. Ribosomal subunits for Raman spectroscopy were dialyzed exhaustively at 4°C against Tris HCl, pH 7.4, containing the indicated concentrations of Mg<sup>2+</sup> or EDTA.

The Mg<sup>2+</sup> content of buffers and ribosomes was measured with an Instrumentation Lab., Inc. flame photometer. Standard curves were constructed using dry Mg<sup>2+</sup> dissolved in 1 N HCl or MgCl<sub>2</sub> dissolved in H<sub>2</sub>O.

### Laser-Raman Spectroscopy

Raman samples (2% ribosomes by weight) were illuminated in Kimax-51 melting point capillaries with the 488 nm line of a Spectra-Physics 165 Ar-ion laser at a constant power of 250 mW at the sample. The scattered light was integrated with a Spex 1400 holographic, double-grating spectrometer equipped with a cooled RCA31034A-02 phototube and Ortec photon counting equipment. Spectra were displayed on a Tektronix 4051 Graphic Display System and a Gould Brush 110 strip chart recorder. Resolution of the spectra were nominally 8 cm<sup>-1</sup>. Peak heights on the spectra were measured from a tangent to the baseline. Raman samples were dialysed extensively against buffers containing 20 mM Tris HCl pH 7.4 and the indicated concentration of EDTA or Mg<sup>2+</sup> at 4°C.

In order to compare different Raman spectra quantitatively it is necessary to normalize peak intensities for differences in nucleic acid concentration and laser power. Most investigators (9-10) have chosen to use the intensity of the 1100 cm<sup>-1</sup> peak (phosphate dioxy stretch) as a normalization factor, since it is expected to be proportional to nucleic acid concentration (one PO<sub>2</sub> group per nucleotide) and since it does not vary with nucleic acid conformation. Since the 1100 cm<sup>-1</sup> intensity varies with Mg<sup>2+</sup> concentration (Fig. 1), however, it is not an ideal standard for

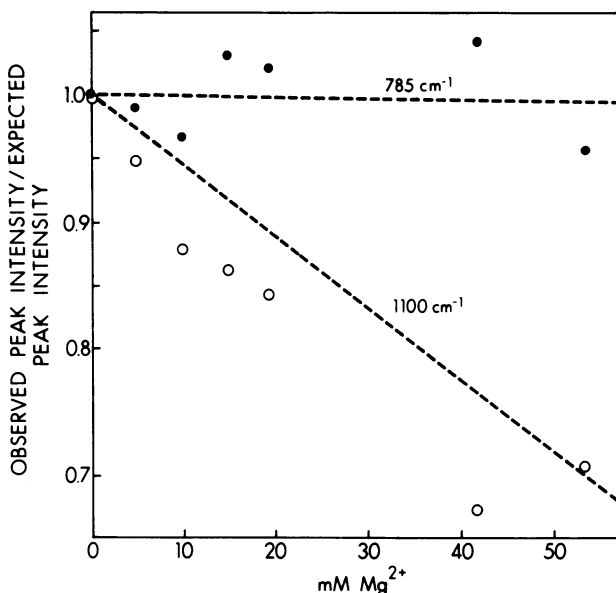


Fig. 1. Relative intensity of 1100  $\text{cm}^{-1}$  and 785  $\text{cm}^{-1}$  signals from 23S rRNA as a function of  $\text{Mg}^{2+}$  concentration.  $\text{Mg}^{2+}$  was added in small aliquots to a solution of 23S RNA, Raman spectra were obtained after each addition and the theoretical dilution of the RNA in the sample was calculated. The 1100  $\text{cm}^{-1}$  and 785  $\text{cm}^{-1}$  peak intensities determined from these spectra divided by the theoretical dilution are plotted as a function of  $\text{Mg}^{2+}$  concentration. Curves are drawn using slopes obtained by linear regression of the experimental points. The intensity of the 785  $\text{cm}^{-1}$  does not depend on  $\text{Mg}^{2+}$  concentration (slope = 0) whereas the intensity of the 1100  $\text{cm}^{-1}$  peak does depend on  $\text{Mg}^{2+}$  concentration (slope not equal to 0).

these studies. Instead, the intensity of the 785  $\text{cm}^{-1}$  peak has been used, since it is independent of the  $\text{Mg}^{2+}$  concentration (Fig. 1). Because the 785  $\text{cm}^{-1}$  vibration arises from cytosine and uracil (9), its intensity depends on the base composition of the nucleic acid studied. However, because only nucleic acids of identical base composition are compared here, it is an adequate normalization standard.

#### Electron Microscopy

The  $\text{Mg}^{2+}$  concentration of the buffer used to adsorb ribosomal subunits to grid support films significantly altered the efficiency of this attachment. In order to minimize differences in binding efficiency when different  $\text{Mg}^{2+}$  concentrations were studied, subunits were attached to grids in 0.2 mM  $\text{Mg}^{2+}$  and subsequently treated with solutions of different

Mg<sup>2+</sup> concentration. Similar results were obtained when subunits were attached to grids in buffers of different Mg<sup>2+</sup> concentrations.

Ribosomal subunits were diluted to a final concentration of 0.5 to 1.0  $\mu\text{g/ml}$  in 20 mM Tris HCl pH 7.4, 0.2 mM MgCl<sub>2</sub> at 25°C. Freshly prepared Parlodion coated grids were touched to the surface of a 100  $\mu\text{l}$  droplet of the subunit suspension, rinsed briefly in 20 mM Tris HCl pH 7.4, and then floated on a droplet of 20 mM Tris HCl pH 7.4 containing the indicated concentration of Mg<sup>2+</sup> or EDTA for 5 or 45 minutes at 25°C. The grids were stained by immersion in 0.05% aqueous uranyl acetate for 30 sec, rinsed for 10 sec in 90% ethanol, blotted, and air dried. Most grids were subsequently rotary-shadowed with tungsten at an incident angle of 8°.

Two parameters of unfolded ribosomal subunits were measured from electron micrographs in order to characterize ribosome unfolding at different Mg<sup>2+</sup> concentrations. First, the maximum diameter of particles was measured by determining the smallest diameter circle into which each particle could be fit (using a circle gauge with increments of one-tenth inch). The diameters obtained were used to construct histograms. Second, particles were classified into shape categories by inspection (see Results).

## RESULTS

### i) Raman detects unfolding

Raman spectra of RNA include a strong vibration at 813 cm<sup>-1</sup> which is correlated with nucleic acid conformation (10). The 813 cm<sup>-1</sup> peak arises from the in chain phosphodiester (O-P-O) symmetric stretch when the ribose rings of a polynucleotide are in the 3' endo conformation (11). (The intensity of the 813 peak is therefore expected to be proportional to the number of nucleotides in the 3' endo conformation.) If the ribose moieties of a polynucleotide are perturbed from the rigid 3' endo conformation, the O-P-O symmetric stretch vibration is shifted to lower wave numbers (12). As a result, the intensity at 813 cm<sup>-1</sup> is diminished. The dependence of the intensity at 813 cm<sup>-1</sup> on the 3' endo conformation is predicted by theoretical calculations (11) and has been demonstrated by comparison of LR spectra of DNA in the A form (3' endo, where the 813 cm<sup>-1</sup> peak is present) and in the B form (3' exo, where the 813 cm<sup>-1</sup> peak is absent; ref. 12).

We have defined an ordering parameter " $\gamma$ " by dividing the intensity of the 813 cm<sup>-1</sup> peak by that of the 785 cm<sup>-1</sup> peak (i.e. normalizing the intensity of the 813 peak for nucleic acid concentration, etc.).  $\gamma$  is a sensitive indicator of changes in ribosome structure induced by heating.

Ribosomal subunits are more stable to increases in temperature and melt more cooperatively than their corresponding rRNAs, in agreement with UV and CD data (13). Fig. 2 shows a portion of a spectrum of 50S ribosomes at 25° in 0.2 mM Mg<sup>2+</sup> solution (solid line); the 813 and 785 cm<sup>-1</sup> signals are prominent. When the ribosomes were heated to 60° in 10 mM EDTA, most of the spectral peaks, including that at 785 cm<sup>-1</sup>, were unchanged; but the 813 cm<sup>-1</sup> signal (dashed line, Fig. 2) was essentially absent. We found that the 785 cm<sup>-1</sup> peak intensity did not vary relative to the intensity of the standard peak from cacodylate buffer (10) up to 60°C (data not shown). Others have found that the 785 cm<sup>-1</sup> peak intensity from tRNA increased 16% between 32° and 80°C (14), but even the small changes observed in that case below 60°C (14), would have only a small effect on the value of  $\gamma$  compared to the changes occurring in the 813 cm<sup>-1</sup> peak.

A part of the 813 cm<sup>-1</sup> signal is lost when Mg<sup>2+</sup> is removed from the ribosomes, even at 25°C. Comparison of the  $\gamma$  values of ribosomal subunits at different Mg<sup>2+</sup> concentrations indicates that  $\gamma$  is a sensitive function of Mg<sup>2+</sup> concentration at 25°C (Fig. 3) [unlike UV and CD spectra which show only small changes during ribosome unfolding at 25°C (see Discussion)].

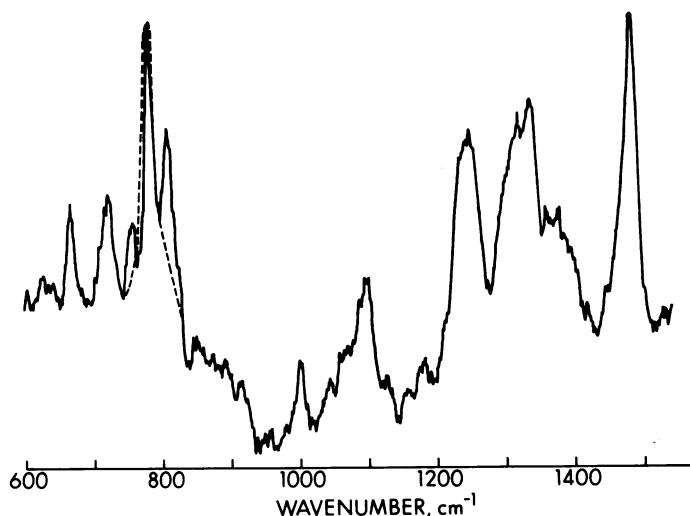


Fig. 2. Raman spectrum of 50S subunits in 0.2 mM Mg<sup>2+</sup> at 25°C (solid line). A portion of a spectrum of subunits in 10 mM EDTA at 60° has been superimposed (dotted line), with the intensity of its 785 cm<sup>-1</sup> peak normalized to that of the subunits in 0.2 mM Mg<sup>2+</sup>, laser power = 300 mW, sample concentration = 2.6%, scan rate = 1 cm<sup>-1</sup> per second, time constant = 3 sec. Slit width = 600/800/600.

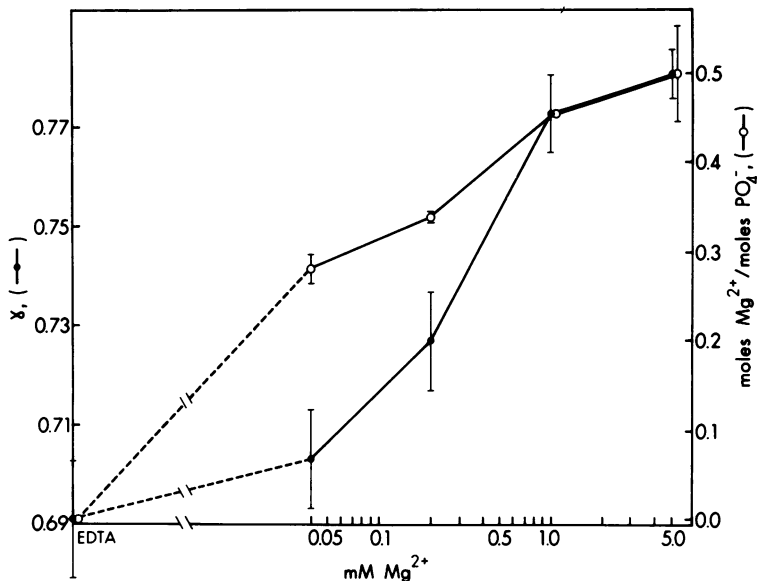


Fig. 3. The  $Mg^{2+}$  content of ribosomes (expressed as moles  $Mg^{2+}$ /moles  $PO_4$ ) and the values of  $\gamma$  for ribosomes as a function of the ambient  $Mg^{2+}$  concentration. The scales have been selected so that the values of  $\gamma$  and moles  $Mg^{2+}$ /moles  $PO_4$  are the same in EDTA and 5 mM  $Mg^{2+}$ . Note that these two parameters deviate from each other maximally when subunits in EDTA are brought to 0.04 mM  $Mg^{2+}$ : the  $Mg^{2+}$  content of ribosomes increases from nearly zero to more than 50% saturation of ribosomal phosphates (one  $Mg^{2+}$  per two  $PO_4$  is complete saturation), while  $\gamma$  increases by only 13% of its total change between EDTA and 5.0 mM  $Mg^{2+}$ . Bars indicate standard errors for six experiments. (Three experiments with 50S and three with 30S ribosomes gave indistinguishable results.)

Changes in  $\gamma$  which occur when  $Mg^{2+}$  is removed from ribosomes, result from changes in the  $813\text{ cm}^{-1}$  peak intensity, since the intensity of the  $785\text{ cm}^{-1}$  peak does not depend on  $Mg^{2+}$  concentration (see Methods). Since the  $813\text{ cm}^{-1}$  peak arises from a phosphate vibration, it is conceivable that the discharge of phosphate groups when  $Mg^{2+}$  is removed from ribosomes could produce changes in  $\gamma$ , independent of changes in ribose conformation. If this were the case, the  $Mg^{2+}$  content of ribosomes at different ambient  $Mg^{2+}$  concentrations would be expected to be proportional to the value of  $\gamma$  at the corresponding  $Mg^{2+}$  concentration. In order to investigate this possibility, we determined the  $Mg^{2+}$  content of ribosomes at different ambient  $Mg^{2+}$  concentrations by flame photometry (see Methods). Fig. 3 demonstrates that these two parameters are not propor-

tional, making it unlikely that  $\gamma$  is only measuring the discharge of phosphate groups.

#### ii) Electron microscopy detects intermediates in unfolding

Electron microscopy revealed large increases in the maximum diameter of ribosomal subunits when they were exposed to EDTA or low  $Mg^{2+}$  concentrations. Histograms representing the distribution of 30S and 50S subunit diameters measured from electron micrographs (see Methods) at different  $Mg^{2+}$  concentrations are presented in Fig. 4. The maximum diameters of 30S and 50S subunits were unaffected (differences not significant by t test) when the  $Mg^{2+}$  concentration was decreased from 1 mM to 0.2 mM. The mean diameters obtained in 0.2 mM  $Mg^{2+}$  (30S = 24 nm, 50S = 24 nm) are in good agreement with estimates of subunit diameter by electron microscopy (15) and low angle X-ray scattering (16). The size distribution of particles was not altered by prolonged incubation in 0.2 mM  $Mg^{2+}$  before staining (data not shown). Decreasing the  $Mg^{2+}$  to 0.04 mM resulted in a time-dependent increase in the maximum diameter of both 30S and 50S subunits (see Fig. 4, panels b and c; f and g). After five minutes in 0.04 mM  $Mg^{2+}$  (see Methods), 34% of the 30S particles examined had diameters greater than two standard deviation units above the mean for 30S particles in 0.2 mM  $Mg^{2+}$  (i.e., 29 nm). After 45 min the diameter of 62% of the 30S particles was greater than 29 nm. The 50S subunit apparently unfolded more rapidly than the 30S subunit in 0.04 mM  $Mg^{2+}$ , since within five minutes 81% of the 50S particles examined had diameters greater than two standard deviation units above the mean for 50S particles in 0.2 mM  $Mg^{2+}$  (i.e., 26 nm).

Both 30S and 50S particles unfolded much more rapidly in 10 mM EDTA than in 0.04 mM  $Mg^{2+}$ . After a 5 min exposure to 10 mM EDTA, none of the particles examined retained the dimensions of native subunits. Furthermore, unfolding was complete after 5 min exposure to 10 mM EDTA, since the mean diameters measured after 5 min (30S = 44 nm; 50S = 58 nm) were little different from those measured after 45 min exposure to 10 mM EDTA (30S = 44 nm; 50S = 54 nm).

In order to define any structural intermediates in the unfolding reaction, ribosomal subunits at different  $Mg^{2+}$  concentrations and in EDTA were classified into six shape categories. The categories were defined as follows: I, round or elliptical particles (i.e. "native" subunits); II, particles with a single projection; III, particles with 2 projections; IV, rod-like particles of uniform width; V, particles with three distinct domains; and VI, particles with four or more distinct domains. Figure 5a

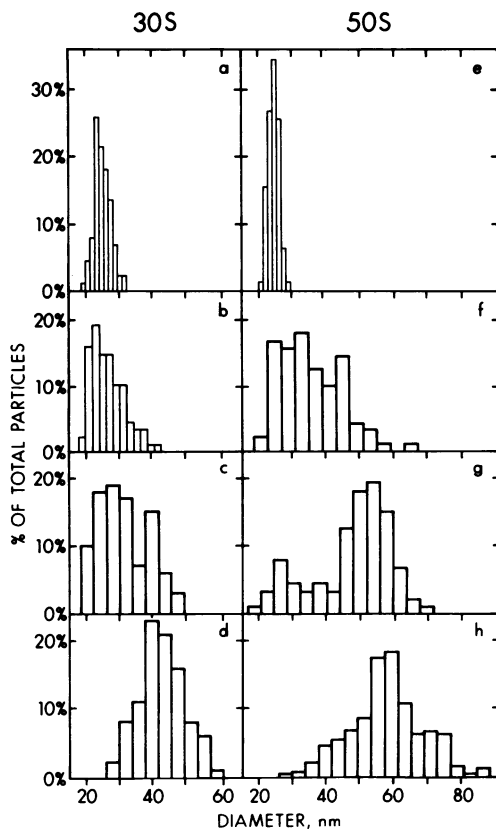


Fig. 4. Histograms representing the percent of particles with particular maximum diameters. Samples were attached to grids in 20 mM Tris HCl pH 7.4 (see text) and were then exposed to the indicated  $Mg^{2+}$  or EDTA concentration for 5 or 45 minutes. Mean diameters ( $\bar{x}$ ) and the number of particles measured ( $n$ ) are indicated for each condition.

a) 30S subunit 0.2 mM $Mg^{2+}$ 5 minutes	$\bar{x} = 24$ nm	$n = 90$
b) 30S subunit 0.04 mM $Mg^{2+}$ 5 minutes	$\bar{x} = 27$ nm	$n = 89$
c) 30S subunit 0.04 mM $Mg^{2+}$ 45 minutes	$\bar{x} = 31$ nm	$n = 100$
d) 30S subunit 10 mM EDTA 5 minutes	$\bar{x} = 44$ nm	$n = 100$
e) 50S subunit 0.2 mM $Mg^{2+}$ 5 minutes	$\bar{x} = 24$ nm	$n = 79$
f) 50S subunit 0.04 mM $Mg^{2+}$ 5 minutes	$\bar{x} = 37$ nm	$n = 89$
g) 50S subunit 0.04 mM $Mg^{2+}$ 45 minutes	$\bar{x} = 47$ nm	$n = 87$
h) 50S subunit 10 mM EDTA 5 minutes	$\bar{x} = 58$ nm	$n = 226$

shows representative particles from each shape class for 30S and 50S subunits (no class III or class VI particles were observed among the 30S subunits at any  $Mg^{2+}$  or EDTA concentration). Fig. 5b shows a field of 50S



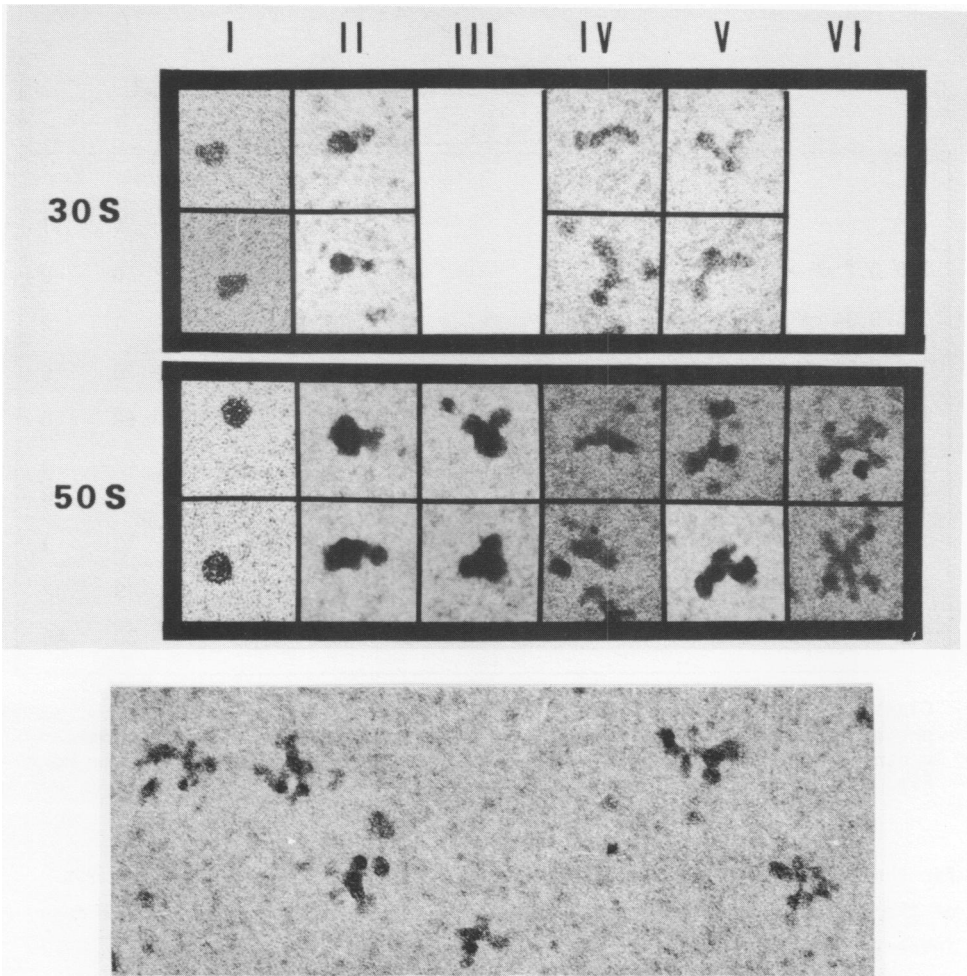


Fig. 5. a. Typical 30S and 50S subunits from each shape class (see text). No 30S particles could be assigned to class III or class VI. Magnification X157,500. b. A field of 50S ribosomes in EDTA, predominantly of class VI. Magnification X156,600

subunits predominantly of class VI. Particles could be classified with little ambiguity; less than 5% of all the particles examined were unassignable, and independent observers agreed on more than 85% of the assignments. The percentage of particles in each shape category is shown in Table I.

Native 30S particles accounted for over 90% of the particles examined in 0.2 mM  $Mg^{2+}$ . After 5 minutes in 0.04 mM  $Mg^{2+}$ , class I still accounted

Table 1  
Distribution of Ribosomes in Electron Micrographs as a  
Function of Mg<sup>2+</sup> Concentration

	Class, as %					
	I	II	III	IV	V	VI
30S 0.2 mM Mg <sup>2+</sup>	90	5	0	5	0	0
30S 0.04 mM Mg <sup>2+</sup> 5 min	56	42	0	1	1	0
30S 0.04 mM Mg <sup>2+</sup> 45 min	19	33	0	28	20	0
30S 10 mM EDTA 5 min	1	10	0	31	58	0
50S 0.2 mM Mg <sup>2+</sup>	96	3	0	0	1	0
50S 0.04 mM Mg <sup>2+</sup> 5 min	39	18	21	9	10	3
50S 0.04 mM Mg <sup>2+</sup> 45 min	18	12	27	13	18	12
50S 10 mM EDTA 5 min	0	5	11	14	30	40

Class I particles are native subunits; II, particles with a single projection; III, with 2 projections; IV, rod-like particles of uniform width; V, with 3 distinct domains; VI, with 4 or more distinct domains (see Fig. 5).

for the majority of 30S particles observed; but after 45 min less than 20% of the particles were assigned to class I. Class II 30S particles were found infrequently in 0.2 mM Mg<sup>2+</sup>, but accounted for more than 40% of the particles examined after 5 minutes exposure to 0.04 mM Mg<sup>2+</sup>. Class II particles were found less frequently after 45 minutes in 0.04 mM Mg<sup>2+</sup>, and accounted for less than 10% of the particles examined in 10 mM EDTA. Class IV and V 30S particles first appeared after 45 minutes in 0.04 mM Mg<sup>2+</sup>, becoming the predominant species in 10 mM EDTA (89%).

Native 50S particles (class I) were the major species in 0.2 mM Mg<sup>2+</sup> (96%), but were found with decreasing frequency after 5 and 45 minutes in 0.04 mM Mg<sup>2+</sup>; and in 10 mM EDTA, no class I particles were observed. Class II and III particles were rare in 0.2 mM Mg<sup>2+</sup> but accounted for a significant fraction of the particles examined in 0.04 mM Mg<sup>2+</sup> (30% jointly). Class II and III particles were less than one-half as frequent in 10 mM EDTA as in 0.04 mM Mg<sup>2+</sup>. Class IV particles were absent in 0.2 mM Mg<sup>2+</sup> but

formed a small fraction of the particles observed in both 0.04 mM  $Mg^{2+}$  and in 10 mM EDTA (10–15%). Class V and VI particles appeared after 5 minutes in 0.04 mM  $Mg^{2+}$  and accounted for an increasing fraction of the particles observed after 45 min in 0.04 mM  $Mg^{2+}$  (30%) and in 10 mM EDTA (70%).

## Discussion

### i) Raman spectroscopy compared to other optical techniques

Raman melting curves ( $\gamma$ ) of ribosomal subunits and rRNA at different  $Mg^{2+}$  concentrations closely parallel CD melting curves (i.e.,  $\theta_{265}$ , the change in ellipticity with temperature at 265 nm) (4), implying that Raman and CD spectra are sensitive to the same types of conformational changes in RNA. However, when EDTA is added to native ribosomes at 25°C, there is no change in  $\theta_{265}$ , although the peak shifts 3 wave numbers higher (4–5). In contrast  $\gamma$  decreases 11% in corresponding conditions (Fig. 3). (There is a much larger change observed by both techniques if EDTA is added to native ribosomes at 37°C). These results seem inconsistent with the notion that Raman and CD measure identical aspects of RNA conformation. However, the observations are self consistent if the CD results are interpreted as suggested by Yang and Samejima (17). They argue that a constant value of  $\theta_{265}$  indicates that the number of bases in a stacked conformation is constant, and that a red shift of the 265  $cm^{-1}$  peak implies that the hydrogen bonds between base pairs have been broken. Raman theory implies that a decrease in the intensity of the 813  $cm^{-1}$  peak (a decrease in  $\gamma$ ) indicates that some nucleotides have been disrupted from the 3' endo conformation. A decrease in  $\gamma$ , however, does not necessarily imply that any bases have been unstacked. Taken together, the Raman and CD results are consistent with the breaking up of base pairs in some rRNA helices during unfolding, with a change in the ribose conformation of the involved nucleotides, but without base unstacking. This interpretation is also consistent with UV absorption data (6), which demonstrate no change in absorbance at 260 nm during unfolding, and only a small (1–2%) hyperchromic effect at 280 nm, implying little or no base unstacking.

Whether or not this suggested interpretation of the spectral data is correct, the LR data presented here imply that a substantial number of nucleotide residues in rRNA are disturbed from the 3' endo conformation during ribosome unfolding. Significantly, the greatest change in  $\gamma$  observed under the conditions studied (10 mM Tris HCl, 25°C) occurred between 0.2 mM and 0.04 mM  $Mg^{2+}$ , rather than between 0.04 mM  $Mg^{2+}$  and EDTA. This

implies that RNA structure was significantly "relaxed" before the amount of bound  $Mg^{2+}$  was reduced below 50% saturation of ribosomal phosphates (a ratio of 0.25 in Fig. 3).

ii) EM compared to sedimentation results

Since RNase I minus strains were not available when  $Mg^{2+}$  depleted ribosomes were first examined by electron microscopy (18), ribonuclease activation resulted in extensive degradation of the unfolded particles. Although a loosening and unfolding of ribosome structure was apparent in those studies, sample degradation precluded any detailed analysis of the unfolding. In another study, when partially deprotonated 50S subunits from *B. subtilis* were depleted of  $Mg^{2+}$ , they became elongated with a two-fold increase in maximum diameter (19). No specific structural features of the unfolded 50S subunits were noted, however.  $Mg^{2+}$  depleted mammalian ribosomes also showed an increase in maximum diameter over native subunits (20,21), with a suggestion of threadlike extensions from unfolded 60S subunits (20). These projections may be comparable to those seen here with class II and III particles.

Since the sedimentation coefficient of a spherical particle is inversely proportional to its Stokes radius, it is possible to compare the sedimentation coefficients of unfolded ribosomes with the diameters measured from electron micrographs. If the native 50S subunit corresponds to a particle with a diameter of 24 nm (measured from electron micrographs of particles in 0.2 mM  $Mg^{2+}$ ), completely unfolded 50S subunits observed at 21S by Gesteland (1) would have a diameter of 57 nm. Analogously, completely unfolded 30S subunits observed at 16S would have a diameter of 45 nm. Comparison of these calculated diameters with Fig. 4 indicates excellent agreement between the diameters calculated for the completely unfolded subunits and those measured in 10 mM EDTA (30S mean diameter = 44 nm, 50S mean diameter = 58 nm). Other sedimentation analyses (22-24), using conditions less similar to those used here, agree substantially with Gesteland's results and with the results presented here.

Gesteland (1) also observed discrete intermediates in the unfolding process, sedimenting at 36S for the 50S and 26S for the 30S subunit. There are no maxima in the histograms that might correspond to such intermediates; rather, particle diameters show a very broad distribution (Fig. 4). However, asymmetric intermediates could sediment homogeneously but bind to EM grids in different orientations, leading to variable measurements of their maximum diameter.

Support for this possibility comes from the analysis of the shapes of particles observed during unfolding in 0.04 mM  $Mg^{2+}$  and EDTA solutions. For example, as Table I and Fig. 5 indicate, after 5 min in 0.04 mM  $Mg^{2+}$ , a major fraction of 30S subunits appear in class II (which has a single projection). Such particles are virtually absent after comparable incubations in 0.2 mM  $Mg^{2+}$  and in 10 mM EDTA (Table I). Their selective presence at an intermediate  $Mg^{2+}$  level is consistent with the possibility that class II particles are intermediates in the unfolding of 30S subunits. Similarly, the progressive increase in frequency of class IV and V particles as the  $Mg^{2+}$  concentration is decreased (or as the incubation in 0.04 mM  $Mg^{2+}$  is prolonged) is consistent with their being final products of the unfolding reaction.

A hypothetical unfolding scheme for the 30S subunit would then have class I particles (Fig. 5) giving rise to one projection (class II), and then opening further to produce classes IV and V.

A basically similar argument holds for the 50S ribosome, for which class II and class III particles are much more common in 0.04 mM  $Mg^{2+}$  than in 0.2 mM  $Mg^{2+}$  or in EDTA; and class V and class VI particles become increasingly more frequent at low  $Mg^{2+}$  concentrations. A possible unfolding scheme would then start from class I particles, which form either one (class II) or two (class III) projections, and then open further to give rise to class V and VI particles.

Class IV particles, which are a major form of unfolding 30S ribosomes, are much less frequent in preparations of unfolding 50S ribosomes. Those observed are smaller than other particles, and are rare with subunit preparations (like that in Table I) in which greater than 85% of the 23S rRNA is intact. In contrast, with 50S ribosome preparations in which a break has occurred near the middle of most 23S rRNA molecules, class IV particles are much more frequent, and few class VI particles are seen (data not shown). It seems likely that class IV 50S particles are fragments of the ribosomes similar to those obtained by partial nuclease digestion (25).

Of course the results do not establish these unfolding pathways as correct; class I particles could, for example, proceed directly to class V or VI. It should be possible to assess the unfolding pathway more accurately by defining more precisely the kinetics of unfolding in 0.04 mM  $Mg^{2+}$ , and by examining the distribution of r-proteins in the putative intermediates using monoclonal antibodies (26). Such studies might help to test the speculative possibility that the domains of structure suggested for

unfolded subunits may correspond to the domains of secondary structure predicted for rRNA (27).

It is of some interest that native ribosomes were observed to reach almost the same EM configuration and Raman spectrum in 0.04 mM  $Mg^{2+}$  as in 10 mM EDTA (Figs. 1, 3-4, Table 1, and unpublished data). These results imply that ribosomes can be unfolded to the same determined structure when only a fraction of bound  $Mg^{2+}$  ions are displaced (i.e. 50%). In our experiments—at 25° in 20 mM Tris HCl, pH 7.6—0.04 mM  $Mg^{2+}$  was a critical  $Mg^{2+}$  concentration for ribosome structure; but the minimum level of  $Mg^{2+}$  required to maintain ribosomes as native subunits depends on other variables as well as  $Mg^{2+}$  concentration, including temperature and ionic strength (1, 13, 22).

Since EM and Raman measurements of ribosome unfolding are correlated with regard to the  $Mg^{2+}$  concentration at which changes occur, it is likely that the two techniques measure similar phenomena or different aspects of the same phenomenon. Kinetic Raman studies would further elucidate this relationship by showing whether these techniques are correlated with regard to time course as well as  $Mg^{2+}$  concentration. Although only the 813  $cm^{-1}$  Raman peak was observed to change with ribosome unfolding in this study, spectral data already indicate that some other rRNA peaks also change in intensity. Indeed, if the sensitivity of Raman spectra were significantly improved, it might be possible to study changes in r-protein peaks which are now undetectable because of the much more intense rRNA peaks.

### ACKNOWLEDGEMENTS

This research was supported by a grant from the National Science Foundation, and by NIH-NRSA GM 07200 fellowship support for T.C.K.

### REFERENCES

1. Gesteland, R.F. (1966) *J. Mol. Biol.*, 18, 356-371.
2. Tal, M., (1974) *Biochim. Biophys. Acta* 195, 76-86.
3. Gabler, R., Westhead, E.W., and Ford, N.C. (1974) *Biophysical J.*, 14, 528-545.
4. Adler, A.J., Fasman, G.D., and Tal, M. (1970) *Biochim. Biophys. Acta* 213, 424-436.
5. Wong, K.P., and Dunn, J.M., (1974) *FEBS Letters* 44, 50-54.
6. Belli, M., Onori, G., Araco, A., and Giorgi, C. (1976) *Biopolymers* 15, 1229-1232.
7. Luoma, G.A., and Marshall, A.G., (1978) *Proc. Natl. Acad. Sci. U.S.A.* 75, 4901-4905.
8. Noll, M., Hapke, B., Schreier, M.H., and Noll, H. (1973) *J. Mol. Biol.* 75, 281-294.

9. Thomas, G.J., Prescott, B., McDonald-Ordzie, P.E., and Hartman, K.A. (1976) *J. Mol. Biol.* 102, 103-124.
10. Small, E.W., and Peticolas, W.L. (1971) *Biopolymers* 10, 69-88.
11. Brown, E.B., and Peticolas, W.L. (1975) *Biopolymers* 14, 1259-1271.
12. Erfurth, S.C., Kiser, E.J., and Peticolas, W.L. (1972) *Proc. Natl. Acad. Sci. U.S.A.* 69, 938-941.
13. King, T.C., Schlessinger, D., and Milanovich, F. (1980) *Biophysical J.* 32, 456-458.
14. Chen, M.C., and Thomas, G.J. (1974) *Biopolymers*, 13, 615-626.
15. Lake, J.A. (1976) *J. Mol. Biol.* 105, 131-159.
16. Hill, W.E., Thompson, J.O., and Anderegg, J.W. (1969) *J. Mol. Biol.* 44, 89-102.
17. Yang, J.T., and Samejima, T. (1969) in *Prog. Nucleic Acid Res. and Molec. Biol.*, Davidson, I.N. and Cohn, W.E. Eds. Vol. 9, 223-300, Academic Press, New York.
18. Spirin, A.S., Kisselev, N.A., Shukulov, R.S., and Bogdanov, A.A. (1963) *Biokhimiya*, 28, 920-930.
19. Nanninga, N. (1970) *J. Mol. Biol.* 48, 367-371.
20. Haga, J.Y., Hamilton, M.G., and Petermann, M.L. (1970) *J. Cell. Biol.* 47, 221-221.
21. Bielka, H., Wahn, K., Noll, F., and Lutsch, G. (1972) *Acta Biol. Med. Germ.* 29, 607-619.
22. Gavrilova, L.P., Ivanov, D.A., and Spirin, A.S. (1965) *J. Mol. Biol.* 16, 473-489.
23. Cammack, K.A., and Wade, H.E. (1965) *Biochem. J.* 96, 671-680.
24. Miall, S.H., and Walker, I.O. (1969) *Biochim. Biophys. Acta* 174, 551-560.
25. Spitnik-Elson, P. and Elson, D. (1979) *Methods in Enzymology* 59, 461-481.
26. Shen, V., King, T.C., Kumar, V., and Daugherty, B. (1980) *Nucleic Acid Res.* 8, 4639-4649.
27. Noller, H.F. (1980) In *Ribosomes: Structure, Function, and Genetics*, Chambliss, G., Craven, G.R., Davies, J., Davis, K., Kahan, L., and Nomura, M., Eds., 3-22, Univ. Park Press, Baltimore.